

Division - Soil In Space and Time | Commission - Soil Survey and Classification

Gypsic soils in the Brazilian Semiarid

Artur Henrique Nascimento da Silva⁽¹⁾ , Marilya Gabryella Sousa⁽¹⁾ , José Coelho de Araújo Filho⁽²⁾ , Marcelo Metri Corrêa⁽³⁾ , Xose Lois Otero⁽⁴⁾ , Tiago Osório Ferreira⁽⁵⁾ , Maria Augusta Maciel Alves Correia⁽¹⁾  and Valdomiro Severino de Souza Júnior^{(1)*} 

⁽¹⁾ Universidade Federal Rural de Pernambuco, Departamento de Agronomia, Recife, Pernambuco, Brasil.

⁽²⁾ Empresa Brasileira de Pesquisa Agropecuária, Unidade de Execução de Pesquisa, Recife, Pernambuco, Brasil.

⁽³⁾ Universidade Federal do Agreste de Pernambuco, Centro Acadêmico de Garanhuns, Garanhuns, Pernambuco, Brasil.

⁽⁴⁾ Faculdade de Biología, Universidade de Santiago de Compostela, Departamento de Edafología y Química Agrícola, Santiago de Compostela, España.

⁽⁵⁾ Universidade de São Paulo, Escola Superior de Agricultura Luiz Queiroz, Departamento de Ciência do Solo, Piracicaba, São Paulo, Brasil.

ABSTRACT: Globally, soils with gypsic horizons cover approximately 1 million km², predominantly in arid climates. The formation of pedogenic gypsum in soils has been a topic of discussion in pedological studies for some time, with gypsification representing the process responsible for secondary gypsum accumulation. Even though international classification systems acknowledge the existence of gypsic horizons, there is a paucity of documented evidence concerning their occurrence in Brazilian soils. This study aimed to identify and describe a soil with secondary gypsum accumulation in the Brazilian semiarid region, employing the established criteria for *in situ* identification and classification. The study was conducted on a soil profile in the semiarid region of Pernambuco State, Brazil, that is undergoing salinization. Morphological descriptions of gypsum precipitates and chemical and mineralogical analysis were evaluated for their suitability for characterizing the material. Turbidimetric methods are more suitable for gypsum determination in hypersaline soils, while thermogravimetric analysis is the most accurate method for its mineralogical identification. This study establishes the first national record of gypsification in Brazilian soils and underscores the necessity of incorporating gypsum presence criteria into the Brazilian Soil Classification System (SiBCS) for effective soil management and environmental conservation.

Keywords: salinization, gypsum, soil classification, soil mineralogy, pedogenesis.

* **Corresponding author:**

E-mail: valdomiro.souzajunior@ufrpe.br

Received: July 23, 2024

Approved: November 27, 2024

How to cite: Silva AHN, Sousa MG, Araújo Filho JC, Corrêa MM, Otero XL, Ferreira TO, Correia MAMA, Souza Júnior VC. Gypsic soils in the Brazilian semiarid. Rev Bras Cienc Solo. 2025;49:e0240138.

<https://doi.org/10.36783/18069657rbc20240138>

Editors: José Miguel Reichert  and Pablo Vidal Torrado .

Copyright: This is an open-access article distributed under the terms of the Creative Commons Attribution License, which permits unrestricted use, distribution, and reproduction in any medium, provided that the original author and source are credited.



INTRODUCTION

Gypsification process is responsible for accumulating secondary gypsum ($\text{CaSO}_4 \cdot 2\text{H}_2\text{O}$), whether neoformed or translocated, in the soil (Buol et al., 1997). Soils undergoing gypsification are classified as Aridisols (USDA Soil Taxonomy) and Gypsisols (WRB) (Driessen et al., 2001). These soils cover approximately 1 million km^2 globally and are predominantly found in arid climate zones (Carter and Inskeep, 1988; Herrero et al., 1992; Abdelfattah, 2013; Casby-Horton et al., 2015; Fazeli et al., 2017; Blackburn et al., 2020).

Due to its high solubility, gypsum dissolves readily and its dynamics in soil horizons are typically influenced by water movement. Gypsum accumulation in the soil matrix is dependent on several physical and chemical factors, including soil texture and the levels of Ca^{2+} and SO_4^{2-} present. Gypsum can precipitate in different crystal shapes, with varying chemical compositions and accumulation pedofeatures. Additionally, it can occur in association with other minerals, such as carbonates and soluble salts (Casby-Horton et al., 2015).

Taxonomically, gypsum accumulation results in the formation of gypsic horizons (Schaetzl and Anderson, 2005), which are recognized as a diagnostic feature in the two main international soil classification systems:

Soil Taxonomy: *The gypsic horizon is an illuvial horizon in which secondary gypsum has accumulated to a significant extent. It typically occurs as a subsurface horizon, but it may occur at the surface in some soils* (Soil Survey Staff, 2022).

WRB: *A gypsic horizon (from Greek gypsos, gypsum) is a non-cemented horizon containing accumulations of secondary gypsum ($\text{CaSO}_4 \cdot 2\text{H}_2\text{O}$) in various forms. It may be a surface or a subsurface horizon* (IUSS Working Group WRB, 2022).

In South America, gypsic soils are mainly found in the arid regions of Patagonia (Argentina) and the Atacama Desert (Chile) (Casby-Horton et al., 2015). Marengo and Bernasconi (2015) identified arid-like conditions in Northeast Brazil, which are intensified by processes such as severe droughts and salinization, leading to soil degradation. Given the combination of these climatic factors and the presence of geological sources of gypsum, the extent of gypsic soils in Brazil is expected to be underestimated.

The current edition of the Brazilian Soil Classification System (SiBCS) (Santos et al., 2018) does not acknowledge the presence of gypsic attributes. However, soil surveys have documented indications of gypsum accumulation in Brazilian soils (Schaefer, 2013; Vidal-Torrado et al., 2020).

Furthermore, identifying gypsum in soils is crucial, as it is directly associated with other pedogenetic attributes, including salic, sodic, carbonatic, and thionic (Buol et al., 1997; Schaetzl and Anderson, 2005). These attributes have implications for soil physical and chemical properties, since gypsum affects land use by altering soil porosity, hydraulic conductivity, and nutrient balance (Curtin et al., 1993; Violante et al., 2002; Agbenin, 2003; Rasiyah et al., 2004).

The principal objective of this study was to present the first evidence of secondary gypsum in a soil from the Brazilian semiarid region. The aim was to apply the existing criteria for identifying and classifying gypsic features based on soil morphological description *in situ*. For that purpose, we tested methods and necessary adaptations for gypsum determination and subsequent inclusion of gypsic character into the SiBCS. Different mineralogical methods, including X-ray diffraction, differential thermal analysis, and Fourier transform infrared spectroscopy, were also employed to identify gypsum, providing background for further studies.

MATERIALS AND METHODS

Study site

The study site is situated in the Northeastern region of Brazil, within the municipality of Ibimirim in the state of Pernambuco ($8^{\circ} 32' 02.0''$ S $37^{\circ} 40' 58.8''$ W). The soil was sampled at a distance of approximately 90 m from the Moxotó River in a circular depression with a distinctive micro-relief pattern (Figure 1). The study site is situated in an area characterized by recent alluvial deposits along the floodplain of the Moxotó River. The climate in the area is classified as hot semiarid (Bsh), according to the Köppen classification system, with an average annual rainfall of 576 mm (Campello et al., 2021). The driest months are from May to December, while the hottest months are from September to April, with a mean temperature of 27°C .

The region is lithologically characterized by the presence of the Jatobá sedimentary basin, which dates to the Paleozoic and Mesozoic eras. This basin is composed of fine to medium-grained sandstones, shales, and siltstones. Additionally, occurrences of laminated limestones and gypsum facies are present in smaller proportions (Neumann, 2017).

During the sampling process, the field observation revealed a considerable accumulation of salts on the soil surface, accompanied by a notable reduction in plant density compared to the surrounding areas (Figure 1). The few species that were able to establish themselves in the soil surroundings were small strata, including Reloginho (*Sida spinosa*), Pegapinto (*Boerhavia diffusa* L.), and Vassourinha (*Scoparia dulcis*). Additionally, some tree species in an intermediate stage of succession, such as Feijão-Bravo (*Capparis hastata*) and exotic species Algaroba (*Prosopis juliflora*), were observed at the site.

Gypsum efflorescence description and sampling

A soil trench was excavated manually (Figure 2). The morphological description of the soil was conducted in accordance with the World Reference Base (WRB) (IUSS Working Group WRB, 2022) and in alignment with the methodology proposed by Santos et al. (2015). A detailed description of the salt precipitates was made based on their percentages and sizes, adapting the charts to describe mottles (Santos et al., 2015) and their morphology according to the WRB (IUSS Working Group WRB, 2022).

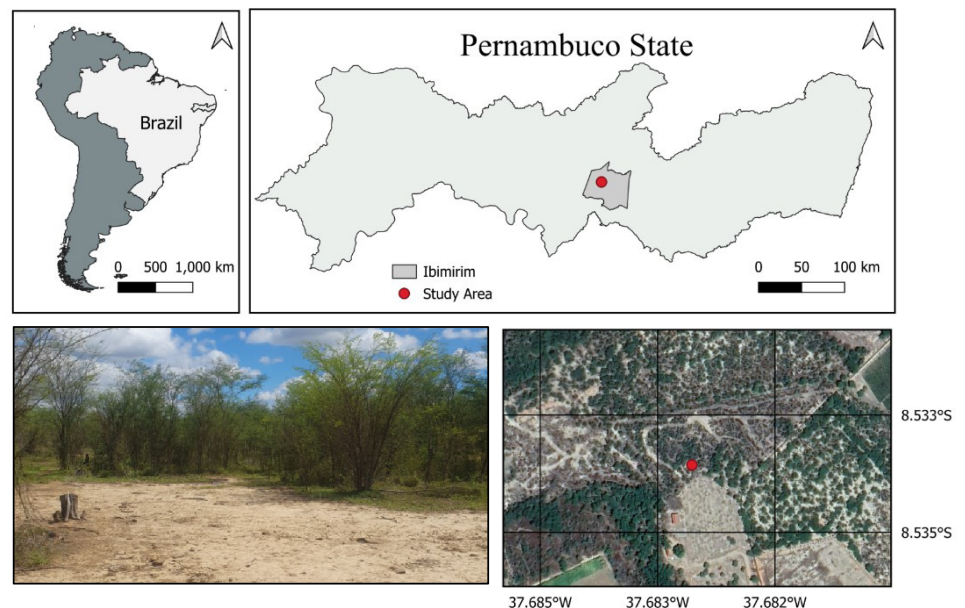


Figure 1. Location of the study area in Ibimirim, Pernambuco, Brazil.

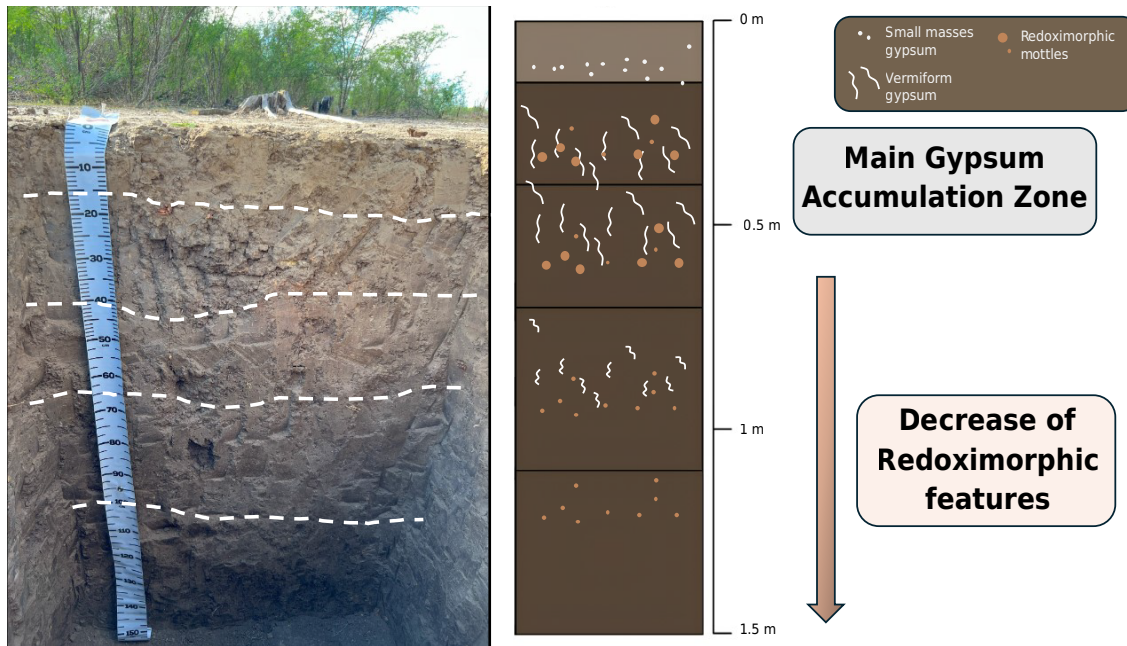


Figure 2. Representative hypersaline soil profile in Ibimirim, Pernambuco, Brazil, and visual representation of the soil profile highlighting the regions and dynamics of gypsum precipitation and accumulation, as well as redoximorphic features.

Aggregates with salt efflorescences were also selected for morphological characterization, employing a petrographic microscope, and a scanning electron microscope equipped with an energy-dispersive X-ray microprobe (SEM-EDX).

Subsequently, a methodology for gypsum field testing of gypsum was conducted. Aggregates with salt precipitates were selected and manually disaggregated, and approximately 5 g was added to a 45 mL tube. A volume of 30 mL of distilled water was added, followed by manual shaking for approximately 2 min. The extract was filtered through quantitative filter paper. Three drops of barium chloride (BaCl_2) at a concentration of 10 % were added, and the formation of whitish turbidity corresponding to barium sulfate was observed.

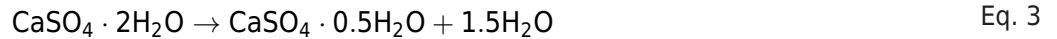
This method was adapted from the quantitative laboratory determination method for gypsum proposed by Richards (1954). It involves the reaction of gypsum with water (Equation 1) and subsequent barium sulfate precipitation, which is easily visible (Equation 2).



Quantitative determination of gypsum

To determine the total gypsum content, three distinct methods were employed following the protocol outlined by Álvarez et al. (2022). The initial method employed was thermogravimetric analysis (TGA), which involves the quantification of mass loss resulting from the dehydration of water molecules present in the mineral ($\text{CaSO}_4 \cdot 2\text{H}_2\text{O}$) at temperatures between 100 and 150 °C (Poch, 1992).

Approximately 20 mg of previously dried soil was subjected to heating from 25 to 500 °C at a rate of 10 °C/min under a nitrogen gas atmosphere, using a Netzsch STA 449 F3 instrument. Gypsum quantification was performed based on the mass losses observed between 120 and 150 °C, which correspond to the dehydration of the mineral in two steps (Equations 3 and 4) (Földvári, 2011).



The second method employed a temperature range of 70–105 °C. The fundamental principles of this method are analogous to those of TGA analysis, entailing gravimetric assessment at fixed temperatures (for further details, see Artieda et al., 2006). Approximately 10 g of soil were subjected to heating in a muffle furnace at 70 °C for 48 h to promote the loss of hydration water from the soil. Following this, the samples were weighed on an analytical balance. Subsequently, the samples were heated again at 105 °C for the same period to promote gypsum dehydration.

A turbidimetry method was ultimately employed. Prior to analysis, soil samples were subjected to a pretreatment involving the use of 97 % alcohol, which was effective in achieving the complete removal of chlorides and sulfates, until the tests with silver nitrate (3 % AgNO₃) and barium chloride (10 % BaCl₂) yielded negative results, in accordance with the methodology described by Richards (1954). Subsequently, 250 mL of deionized water (1:50 ratio) were added, followed by agitation for 8 h (Álvarez et al., 2022) and centrifugation at 3500 rpm for 25 min. Next, 50 mL of the aqueous extract were utilized to ascertain the sulfate content via turbidimetry, employing a spectrophotometer at 420 nm (BEL Photonics - Spectrophotometer SP 1105) in accordance with the methodology proposed by Porta (1998).

Mineralogical analyses

Gypsum efflorescences were manually scraped using a metal spatula. The resulting material was pulverized, homogenized in an agate mortar, and passed through a 100-mesh sieve. X-ray diffraction (XRD) was conducted using a Shimadzu XRD-6000 instrument, operating with a tube that emitted Cu-K α radiation at a voltage of 40 kV and a current of 30 mA, equipped with a graphite monochromator. The sample was prepared as an unoriented powder on a platinum sample holder at a speed of 1 °C/min, with 2 θ recording amplitudes ranging from 3° to 70° (2 θ). Identification was conducted in accordance with the methods of Brown and Brindley (1980) and Moore and Reynolds (1989).

Thermogravimetric analysis (TG) was conducted using a Netzsch STA 449 F3 instrument with the following configuration: the sample was heated from 25 to 1,100 °C at a rate of 10 °C/min under a nitrogen gas atmosphere. The results were interpreted using Proteus[®] Version 5.1 software from Netzsch to generate mass loss curves (TG analysis). The first derivative of the TG curves (DTG) was employed to enhance the visualization of peaks associated with hydration water and structural water loss events. Pattern identification was conducted in accordance with the methodology described by Földvári (2011).

Attenuated Total Reflectance Fourier Transform Infrared (FTIR-ATR) analysis was conducted using a PerkinElmer FT-IR Spectrometer (Spectrum Two), with the *UATR-Two* accessory comprising a diamond crystal operating in the transmission mode. The following conditions were employed: scanning range from 400 to 4000 cm⁻¹, resolution of 4 cm⁻¹, accumulation of 50 scans, and interval of 1 cm. In this test, samples of selected gypsum aggregates were subjected to analysis and a sample of bulk soil for comparison.

RESULTS

Gypsum macro and micromorphological features

During the morphological description (Table 1), the presence of precipitates corresponding to gypsum was observed in the majority of soil horizons. The accumulation is observed

at the interface between the A and B horizons, manifesting as small, rounded masses (Figure 3). These masses exhibit a color range between 2.5YR 8/1 (white) and 2.5YR 8/2 (pinkish white), with a relative abundance of approximately 5 % (Table 2). The aggregates were tested with hydrochloric acid (10 %), but the observation of effervescence was weak and unclear in most attempts. Therefore, it was concluded that the presence of carbonates was minimal.

The most pronounced accumulation of gypsum (up to 10 %) occurs in the B horizon (Figure 3), primarily as biopores channels fillings, which are referred to as vermiform in the IUSS Working Group (IUSS Working Group WRB, 2022).

Microscopic observation revealed the presence of shiny crystals, reaching up to sand-sized particles (Figures 4a and 4b). Further examination with an electron microscope confirmed that the crystals exhibited a high degree of selection, predominantly displaying pseudo-hexagonal and tabular morphologies.

Table 1. Morphological properties and granulometric composition of sampled soil, in Ibimirim, Pernambuco, Brazil

Horizon symbol	Layer	Boundaries ⁽¹⁾	Structure ⁽²⁾	Consistency ⁽³⁾			Granulometric composition				Texture
				Dry	Moist	Wet	Fine sand	Coarse sand	Silt	Clay	
	m			g kg ⁻¹							
Anz	0.00-0.15	SG	mo, m/co, abk/sbk	SH	FI	SP	95	29	365	511	Clay
Binyz1	0.15-0.40	SG	vst, co/vc, abk/sbk; st, vc, pr	H	SR	SP	42	24	339	595	Clay
Binyz2	0.40-0.70	SD	st, m/co, abk/sbk	SH	FI	SP	36	21	247	696	Very Clayey
2Cnyz	0.70-1.10	SD	st, m/co, abk/sbk	SH	FI	SP	40	19	302	639	Very Clayey
2Cnz	1.10-1.50 ⁺	-	st, m/co, abk/sbk	SH	FI	SP	63	30	297	610	Very Clayey

⁽¹⁾ Boundaries - SG: smooth gradual; SD: smooth diffuse. ⁽²⁾ Soil structure type - abk: angular block; sbk: subangular blocky; pr: prismatic. Size - m: medium; co: coarse; vc> very coarse. Degree of development - mo: moderate; st: strong; vst: very strong. ⁽³⁾ Consistency - SH: slightly hard; HA: Hard; FI: firm; SR: slightly rigid; SP: slightly plastic. Described according to Santos et al. (2015).

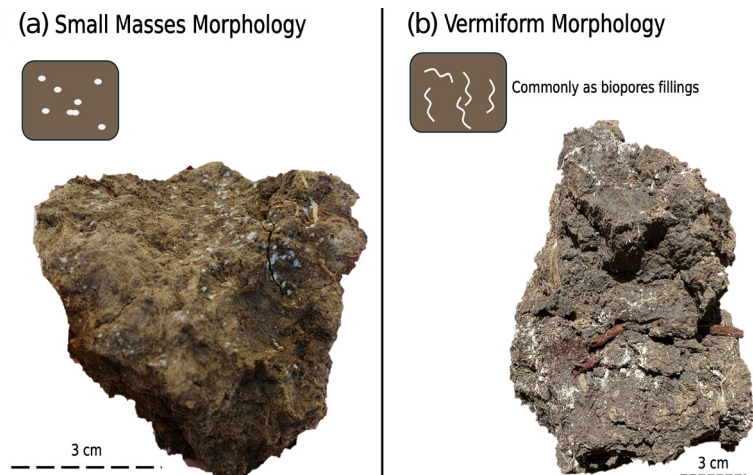


Figure 3. Morphological aspects of gypsum precipitates in the soil structure. (a) Small masses of gypsum precipitate in an angular blocky soil structure. (b) Vermiform gypsum precipitates following the channels of biopores in a prismatic soil structure.

Table 2. Soil color, morphological properties of gypsum precipitates, and redoximorphic mottles of sampled soil, in Ibimirim, Pernambuco, Brazil

Horizon symbol	Layer	Munsell Color (moist)	Mottles			Gypsum		
			Abundance	Color	Size	Location ⁽¹⁾	Abundance	Morphology
	m		%		mm		%	
Anz	0.00-0.15	10YR 5/3		Absent			2-5	Small masses
Binyz1	0.15-0.40	10YR 3/2	10-15	10YR 5/6	6-20	OOH	5-10	Vermiform
Binyz2	0.40-0.70	10YR 3/2	10-15	10YR 5/6	6-20	OOH	5-10	Vermiform
2Cnyz	0.70-1.10	10YR 3/2	10-15	10YR 5/6	6-20	OIB, OOH	2-5	Vermiform
2Cnz	1.10-1.50 ⁺	10YR 3/2	5-10	10YR 5/6	6-20	OIB, OOH		Absent

⁽¹⁾ Mottles location - OOH - Adjacent to surfaces of soil aggregates, infused into the matrix (hypocoats); OIB - Inside soil aggregates: both concretions and/or nodules (not possible to distinguish). Described according to IUSS Working Group WRB (2022).

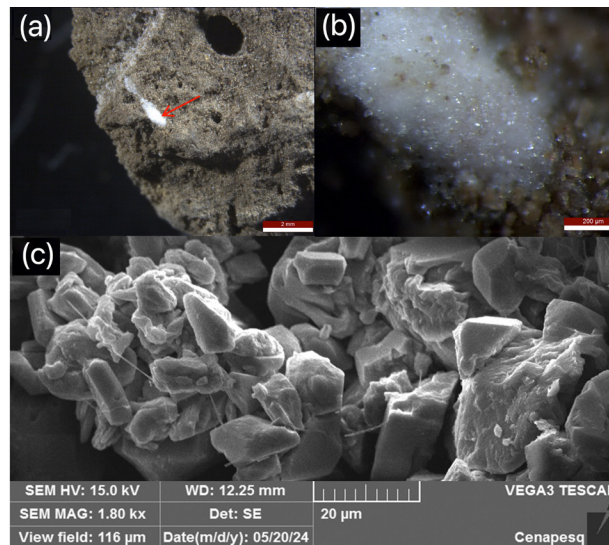


Figure 4. Details of gypsum precipitates. (a) Soil aggregate showing gypsum infilling with vermiform morphology in a biopore (red arrow). (b) The enlargement of the feature observed in image (a), where the aggregation of gypsum crystals is seen. (c) Morphological aspects of the same gypsum crystals under high magnification in an electron microscope, showing a predominance of silt-sized crystals with tabular and pseudo-hexagonal morphology.

Gypsum quantification and mineralogical characterization

Soil chemical attributes are shown in table 3. The results of the thermogravimetric analysis did not indicate the presence of gypsum in the samples. The method proposed by Artieda et al. (2006) revealed a uniform distribution of gypsum throughout the soil profile, with an estimated content of approximately 3 % (Table 4).

Turbidimetry method (Porta, 1998) yielded corroborating values of approximately 3 % (Table 4) in the Bi horizon, where the highest percentage by area was identified macromorphologically. This value decreased to 1.54 % in the deepest horizon.

X-ray diffraction (XRD) analysis revealed the presence of gypsum peaks with interplanar spacings of 0.780, 0.428, and 0.309 nm (Figure 5a). These peaks corresponded to the preferred diffraction planes of this mineral, as previously documented by Fanning et al. (2002).

The FTIR-ATR analysis revealed no statistically significant differences between the interferograms of the two samples (gypsum efflorescence and bulk soil; Figure 5b). The only noticeable distinction was the presence of an asymmetric band between 3560 and 3150 cm^{-1} .

Table 3. Chemical properties of sampled soil, in Ibimirim, Pernambuco, Brazil

Horizon symbol	Layer	pH(1:2.5)		EC	Ca ²⁺	Mg ²⁺	Na ⁺	K ⁺	CEC	ESP	P	TOC
		H ₂ O	KCl									
				dS cm ⁻¹	cmol _c kg ⁻¹					%	mg kg ⁻¹	g kg ⁻¹
CAMBISSOLO FLUVICO Sódico sálico hipogipsíco ⁽¹⁾ (SiBCS) / Fluvic Eutric Cambisol (Clayic, Protogypsic, Salic, Sodic) (IUSS Working Group WRB, 2022)												
Anz	0.00-0.15	6.46	5.98	65.35	32.79	17.12	18.98	4.40	76.65	24.76	4.69	8.88
Binyz	0.15-0.40	7.37	6.66	45.17	33.39	16.69	20.68	0.76	86.64	23.87	1.89	5.87
Binyz2	0.40-0.70	7.63	6.66	36.32	36.31	28.33	16.39	1.07	84.26	19.45	1.87	3.71
2Cnyz	0.70-1.10	7.70	6.52	26.11	31.28	18.67	22.44	1.07	92.06	24.38	1.52	4.42
2Cnz	1.10-1.50 ⁺	8.04	6.69	14.38	29.28	16.91	23.44	1.06	83.96	27.92	1.64	3.78

⁽¹⁾ The terms "sálico" and "hipogipsíco" were included for the taxonomic classification of the studied soil. EC: Electrical Conductivity; CEC: Cation Exchange Capacity; ESP: Exchangeable Sodium Percentage; TOC: Total Organic Carbon.

Table 4. Comparison of chemical analysis for gypsum determination of the hypersaline sampled soil, in Ibimirim, Pernambuco, Brazil

Horizon symbol	Layer	DTA	Artieda	Turbidimetry
			(70 - 105 °C)	
		g kg ⁻¹		
	m			
Anz	0.00-0.15	nd	2.75	0.96
Binyz	0.15-0.40	nd	3.25	3.23
Binyz2	0.40-0.70	nd	3.39	2.42
2Cnyz	0.70-1.10	nd	3.43	1.16
2Cnz	1.10-1.50 ⁺	nd	3.16	1.54
2Cnz	1.10-1.50 ⁺	nd	3.16	1.54

nd: not detected.

Thermogravimetric analysis (TG) revealed an endothermic peak associated with a substantial mass loss at 135 °C (Figure 5c), indicative of dehydration of gypsum (Equations 3 and 4) (Földvári, 2011).

DISCUSSION

Gypsum morphology and accumulation in the soil profile

The observed gypsum precipitation patterns correspond to an initial gypsification process. Some authors consider the occurrence of vermiform morphology observed in the Bi horizon to be analogous to Stage 1 of the calcification process in clayey soils (pseudomycelia morphology) (Neher and Bailey, 1976; Watson, 1979; Carter and Inskeep, 1988).

The images obtained from petrographic and electron microscopes revealed that the precipitated material is distinct from geologically sourced gypsum crystals, which are typically composed of larger and fibrous crystals (Herrero et al., 1992). This also corroborates the hypothesis that the observed gypsum has a pedogenetic origin. The prismatic and columnar crystals observed in this study correlate with those observed in gypsiferous soils from Iran (Jafarzadeh and Burnham, 1992; Hashemi et al., 2011), which are primarily formed under a moisture regime of concentrated rainfall over a short period. This pluviometric pattern is similar to that of the study area.

A parallelism between gypsum accumulation and the presence of redoximorphic features was observed based on an analysis of the accumulation pattern within the profile (Table 2). This pattern strongly suggests that the secondary gypsum formation is linked to hydromorphism and to capillary rise of water (Yamnova and Golovanov, 2010). The

soil is situated close to an active zone of fluvial deposition, and climatically, there is a significant negative water balance (-987 mm), which would favor the upward movement of the water table rich in soluble salts (Reiss et al., 2021).

Therefore, based on the morphological and chemical characteristics observed, the secondary gypsum precipitation in our study is taxonomically consistent with the protogypsic properties described in the WRB (IUSS Working Group WRB, 2022). These properties indicate the gypsum is derived from the soil solution and precipitated within the soil, occupying a minimum of 1 % of the exposed area (without meeting the diagnostic criteria for a gypsic horizon). This differs from gypsum sourced from the soil parent material or other sources, such as dust. Therefore, in the horizon designations, the suffix “y” has been appended where gypsum features were observed (Tables 1, 2, and 3).

Comparison of quantitative and mineralogical methods for gypsum characterization

Thermogravimetric method using DTA proved ineffective in quantifying gypsum. This result is attributed to the small sample size used for analysis, which likely diluted the gypsum with other soil components. It is, therefore, suggested that this analysis may be more effective in soils with higher gypsum contents.

The second quantification assessment, based on the Artieda et al. (2006) method (Table 4), was found to be inconsistent with the field morphology. This is likely attributable to the low accuracy when the gypsum content is below 8 % and to the high expansive and interstratified mineral phases in the soil, which contribute to a high water retention capacity. The absence of notable values between the horizons can be attributed to the fact these minerals necessitate temperatures exceeding 100 °C to achieve complete water removal. Consequently, this leads to interference in the optimal temperature range required for gypsum dehydration (Álvarez et al., 2022).

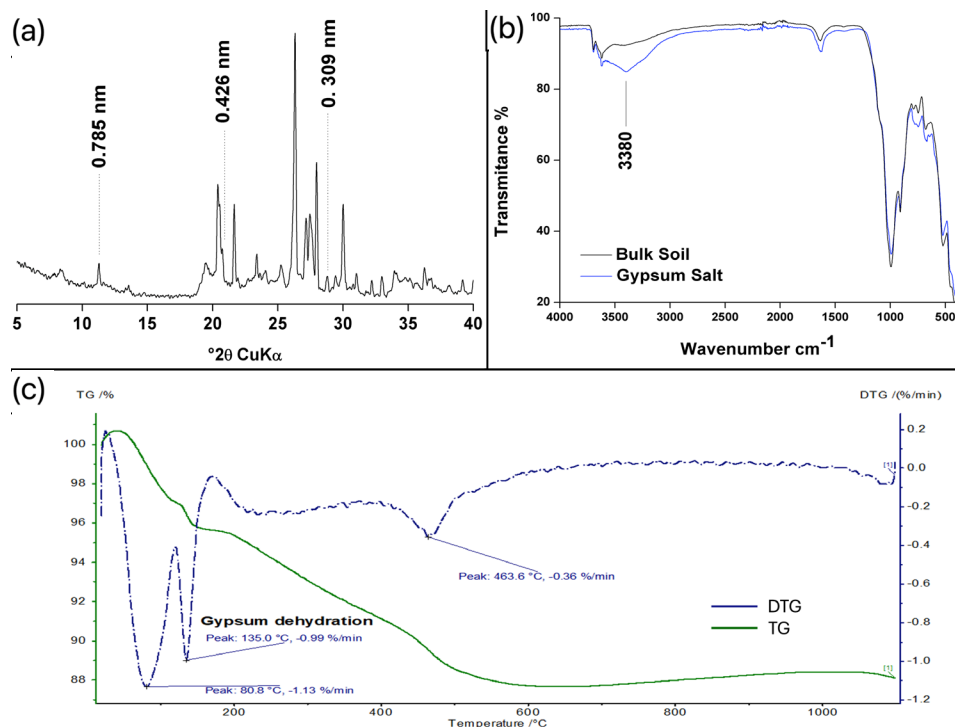


Figure 5. Mineralogical analyses of gypsum using different techniques. (a) X-ray diffractogram of gypsum precipitates, highlighting its diagnostic peaks (0.785, 0.426, and 0.309 nm). (b) Infrared spectrum obtained from the natural soil (black line) and gypsum precipitates (blue line), highlighting the OH-stretching region of the hydration water. (c) TG (green line) and DTG (blue line) curves of gypsum precipitates, highlighting the main mass loss peaks, with the peak at 135 °C corresponding to gypsum dehydration. The remaining peaks correspond to the hydration water of the sample and structural water loss of the dominant minerals in the clay fraction, at 80 and 463 °C, respectively.

Turbidimetry method (Porta, 1998) demonstrates the greatest consistency with the observed field morphology. However, it is important to note that this method determines gypsum indirectly through the sulfate content after its dissolution. In the case of hypersaline soils with a high concentration of soluble sulfates, it is necessary to wash the excess sulfate with alcohol to prevent an overestimation of gypsum.

Diffractograms exhibited pronounced peaks of quartz and feldspar. It is possible that these peaks may interfere with the identification of the 0.428 and 0.309 nm peaks of gypsum (Figure 5a). Therefore, the DTA was the most reliable technique for identifying gypsum, as the derivative plot of the TG curves exhibited anomalous behavior compared to other soils (Figure 5c). Other mass loss peaks at 80 °C correspond to the loss of hydration water in the sample, and an asymmetrical peak at 463 °C represents the expandable and interstratified clay minerals (Karathanasis and Hajek, 1982).

The FTIR-ATR analysis proved to be the least satisfactory among the mineralogical characterization techniques. The bands between 3560 and 3150 cm^{-1} are predominantly associated with OH bonds from water in the samples. Some authors have proposed that they may also be associated with the hydration water calcium sulfate (Wang et al., 2004; Anbalagan et al., 2009). However, given the lack of clarity in the specific sulfate vibration bands, utilizing these FTIR-ATR patterns for gypsum identification would not be optimal.

Agricultural remarks

Soils with elevated soluble salt contents and gypsum precipitates may render these lands unsuitable for agricultural use. The most conspicuous consequences of soil salinization are the restriction of vegetation cover, the accumulation of salts, and the formation of salt crusts (Watson, 1985). In Brazilian soils, salinity is predominantly associated with chloride (Cl^-). There is a paucity of research examining the impact of sulfate (SO_4^{2-}) ions on soil salinity. At the study region, soil samples have been found to contain up to 1,500 mg kg^{-1} of dissolved sulfate in saturation extracts (Pessoa et al., 2019). Sulfate salinization can go unnoticed if not determined, as the electrical conductivity levels for this ion do not behave linearly as for Cl^- ions (Curtin et al., 1993).

Additionally, sulfate has the potential to reduce calcium activity by precipitating CaSO_4 (predominantly gypsum). Among the effects on plants, symptoms of leaf yellowing due to calcium deficiency can be observed (Curtin et al., 1993), as well as a reduction (or even inversion) of the Ca/Mg ratio (Agbenin, 2003). Furthermore, elevated sulfate concentrations can diminish the concentration of phosphates and nitrate ions within the soil exchange complex. This phenomenon is attributed to the competitive adsorption of sulfate over phosphate on soil colloids (Violante et al., 2002; Rasiah et al., 2004).

Gypsum precipitation within soil pores has the potential to impact soil structure, particularly through the phenomenon of gypsoturbation (Casby-Horton et al., 2015). This phenomenon involves a displacive action or expansion resulting from gypsum precipitation, which can lead to the cementation of soil particles and, consequently, a reduction in soil hydraulic conductivity (Watson, 1985).

In the context of the reclamation of salinized areas in the Brazilian semiarid region, leaching is typically associated with the addition of chemical additives, such as agricultural gypsum. Reduction of Cl^- and Na^+ activities, as well as electrical conductivity, has been confirmed in various controlled studies. However, the viability of this strategy in natural conditions is questionable, given these soils exhibit 0 cm h^{-1} of hydraulic conductivity (Ribeiro et al., 1998 a,b; Gheyi et al., 2022). Additionally, the precipitation of secondary gypsum may be intensified by the addition of agricultural gypsum.

Taxonomic suggestion: creation of the “Gypsic character” in the SiBCS

In light of the pivotal role of soil quality in agricultural productivity, it is crucial to consider the implications of gypsification on soil classification. Recent observations at Soil Classification and Correlation Meetings (Schaefer, 2013; Vidal-Torrado et al., 2020) have highlighted the emergence of additional morphological features associated with this process. Therefore, it is important that the Brazilian Soil Classification System (SiBCS) incorporates these observations to ensure comprehensive and accurate soil classification.

The soil described in this research note was classified according to the WRB system regarding gypsum accumulation. This was done to provide information for future updates of the SiBCS and, simultaneously, serve as a starting point for more comprehensive and specific research on the occurrence of soils with an accumulation of “secondary gypsum”. It is recommended that two new characters be created as follows:

The term “Gypsic character” describes the presence of secondary gypsum within the control section that defines the soil class, which is morphologically visible. This secondary gypsum can take a variety of forms and sizes of segregation, and its quantitative value is equal to 50 g kg⁻¹ (or 5 %).

The term “Hypogypsic character” describes the presence of morphologically visible accumulations of secondary gypsum within the control section that defines the soil class. These accumulations may occur in any size or form of segregation, and their quantitative value is less than 50 g kg⁻¹ (5 %) of secondary gypsum.

Both attributes follow a quantitative criterion that can be determined in a laboratory setting, similar to the existing carbonatic and hypocarbonatic characters described in the SiBCS. Both were based on the described gypsic horizon and protogypsic properties from the World Reference Base for Soil Resources, respectively (IUSS Working Group WRB, 2022).

The proposed attributes can be employed to differentiate soil classes at the fourth level of the SiBCS (subgroups). Based on the current knowledge, they are crucial for distinguishing *Vertissolos* (Vertisols), *Neossolo Flúvicos* (Fluvisols), and *Cambissolos Flúvicos* (Cambisols), where evidence of these attributes has already been documented.

CONCLUSIONS

Secondary gypsum is present in soils in the semiarid region of Brazil, exhibiting a sufficient content to identify the protogypsic properties described in the WRB. The presence of secondary gypsum in Brazilian soils should be defined in the SiBCS, as it has been observed under in other Brazilian climates and biomes. The determination of secondary gypsum in hypersaline soils should be based on turbidimetric methods prior to the elimination of soluble salts. The XRD and thermogravimetric analyses were the most accurate mineralogical techniques for identifying secondary gypsum in soils with diverse mineralogical assemblages.

DATA AVAILABILITY

The data will be provided upon request.

FUNDING

This study was supported by the Coordination for the Improvement of Higher Education Personnel (CAPES/Print) - Grant: AUX 88881.163446/2018-01; the National Council for Scientific and Technological Development (CNPq) - Grant: 305916/2023-8; 167925/2022-9

and 313696-2021/7; the Foundation for Support of Science and Technology of the State of Pernambuco (Facepe): Grant: APQ-1356-5.01/21; and APQ-1537-5.01/22; EMBRAPA Solos – Project (10.20.03.032.00.00).

AUTHOR CONTRIBUTIONS

Conceptualization:  Artur Henrique Nascimento da Silva (equal),  José Coelho de Araújo Filho (equal),  Tiago Osório Ferreira (equal),  Valdomiro Severino de Souza Júnior (equal) and  Xose Lois Otero (equal).

Data curation:  Artur Henrique Nascimento da Silva (equal),  José Coelho de Araújo Filho (equal),  Marcelo Metri Corrêa (equal),  Maria Augusta Maciel Alves Correia (equal) and  Marilya Gabryella Sousa (equal).

Formal analysis:  Artur Henrique Nascimento da Silva (equal),  Maria Augusta Maciel Alves Correia (equal) and  Marilya Gabryella Sousa (equal).

Funding acquisition:  José Coelho de Araújo Filho (lead),  Marcelo Metri Corrêa (equal),  Marilya Gabryella Sousa (equal) and  Valdomiro Severino de Souza Júnior (lead).

Investigation:  Artur Henrique Nascimento da Silva (equal),  Maria Augusta Maciel Alves Correia (equal) and  Marilya Gabryella Sousa (equal).

Methodology:  Artur Henrique Nascimento da Silva (equal),  Marcelo Metri Corrêa (equal),  Maria Augusta Maciel Alves Correia (equal) and  Marilya Gabryella Sousa (equal).

Project administration:  Artur Henrique Nascimento da Silva (equal) and  Valdomiro Severino de Souza Júnior (equal).

Supervision:  Valdomiro Severino de Souza Júnior (lead).

Validation:  Artur Henrique Nascimento da Silva (equal),  José Coelho de Araújo Filho (equal),  Marcelo Metri Corrêa (equal),  Tiago Osório Ferreira (equal),  Valdomiro Severino de Souza Júnior (equal) and  Xose Lois Otero (equal).

Writing - original draft:  Artur Henrique Nascimento da Silva (lead).

Writing - review & editing:  Artur Henrique Nascimento da Silva (equal),  José Coelho de Araújo Filho (equal),  Marcelo Metri Corrêa (equal),  Maria Augusta Maciel Alves Correia (equal),  Marilya Gabryella Sousa (equal),  Tiago Osório Ferreira (equal),  Valdomiro Severino de Souza Júnior (equal) and  Xose Lois Otero (equal).

REFERENCES

- Abdelfattah MA. Pedogenesis, land management and soil classification in hyper-arid environments: Results and implications from a case study in the United Arab Emirates. *Soil Use Manage.* 2013;29:279-94. <https://doi.org/10.1111/sum.12031>
- Agbenin JO. Soil saturation extract composition and sulfate solubility in a tropical semiarid soil. *Soil Sci Soc Am J.* 2003;67:1133-9. <https://doi.org/10.2136/sssaj2003.1133>
- Álvarez D, Antúnez M, Porras S, Rodríguez-Ochoa R, Olarieta JR, Poch RM. Quantification of gypsum in soils: Methodological proposal. *Span J Soil Sci.* 2022;12:10669. <https://doi.org/10.3389/sjss.2022.10669>
- Anbalagan G, Mukundakumari S, Murugesan KS, Gunasekaran S. Infrared, optical absorption, and EPR spectroscopic studies on natural gypsum. *Vib Spectrosc.* 2009;50:226-30. <https://doi.org/10.1016/j.vibspec.2008.12.004>

- Artieda O, Herrero J, Drohan PJ. Refinement of the differential water loss method for gypsum determination in soils. *Soil Sci Soc Am J.* 2006;70:1932-5. <https://doi.org/10.2136/sssaj2006.0043>
- Blackburn PW, Fisher JB, Dollarhide WE, Merkler DJ, Chiaretti JV, Bockheim JG. Soil-forming processes in Nevada. In: *The soils of Nevada. World Soils Book Series.* Cham: Springer; 2020. p. 133-6. https://doi.org/10.1007/978-3-030-53157-7_13
- Brown G, Brindley GW. X-ray diffraction procedures for clay mineral identification. In: Brindley GW, Brown G, editors. *Crystal structures of clay minerals and their X-Ray identification.* London: Mineralogical Society; 1980. p. 305-60. <https://doi.org/10.1180/mono-5.5>
- Buol SW, Hole FD, McCracken RJ. *Soil genesis and classification.* 4th ed. Iowa: Iowa State University Press; 1997.
- Campello JLA, Nascimento JS, Barros B, Campello LFM, Ferrari Junior MJ, Sant'anna Filho R. Plano municipal de saneamento básico de Ibimirim - PE. Ibimirim, PE: Instituto de Gestão de Políticas Sociais; 2021 [cited 2024 May 23]. Available from: <https://gesois.org.br/novo/ibimirim/ibimirim%20P2%20Diagnostico%20consolidado.pdf>.
- Carter BJ, Inskeep WP. Accumulation of pedogenic gypsum in Western Oklahoma. *Soil Sci Soc Am J.* 1988;52:1107-13. <https://doi.org/10.2136/sssaj1988.03615995005200040040x>
- Casby-Horton S, Herrero J, Rolong NA. Gypsum soils - Their morphology, classification, function, and landscapes. *Adv Agron.* 2015;10:231-90. <https://doi.org/10.1016/bs.agron.2014.10.0028>. 2015
- Curtin D, Steppuhn H, Selles F. Plant responses to sulfate and chloride salinity: Growth and ionic relations. *Soil Sci Soc Am J.* 1993;57:1304-10. <https://doi.org/10.2136/sssaj1993.03615995005700050024x>
- Driessen P, Deckers R, Spaargaren O, Nachtergaele F. *Lecture notes on the major soils of the world.* Rome: Food and Agriculture Organization of The United Nations; 2001. (World Soil Resources Reports: FAO; Vol. 94).
- Fanning DS, Rabenhorst MC, Burch SN, Islam KR, Tangren SA. Sulfides and sulfates. In: Dixon JB, Schulze DG, editors. *Soil mineralogy with environmental applications.* Madison, WI: Soil Science Society of America, Inc; 2002. p. 229-55.
- Fazeli S, Abtahi A, Poch RM, Abbaslou H. Gypsification processes and porosity changes in soils from southern Iran (Jooyom region-Fars province). *Arid Ecosyst.* 2017;7:80-91. <https://doi.org/10.1134/s2079096117020093>
- Földvári M. *Handbook of thermogravimetric system of minerals and its use in Geological practice.* Budapest: Geological Institute of Hungary; 2011.
- Gheyi HR, Lacerda CF, Freire MBGS, Costa RNT, Souza ER, Silva AO, Fracetto GGM, Cavalcante LF. Management and reclamation of salt-affected soils: General assessment and experiences in the Brazilian semiarid region. *Rev Cienc Agron.* 2022;53:e20217917. <https://doi.org/10.5935/1806-6690.20220058>
- Hashemi SS, Baghernejad M, Khademi H. micromorphology of gypsum crystals in southern Iranian soils under different moisture regimes. *J Agr Sci Tech.* 2011;13:273-88.
- Herrero J, Porta J, Fédoroff N. Hypergypsic soil micromorphology and landscape relationships in northeastern Spain. *Soil Sci Soc Am J.* 1992;56:1188-94. <https://doi.org/10.2136/sssaj1992.03615995005600040031x>
- IUSS Working Group WRB. *World reference base for soil resources. International soil classification system for naming soils and creating legends for soil maps.* 4th. ed. Vienna, Austria: International Union of Soil Sciences (IUSS); 2022. Available from: https://www.isric.org/sites/default/files/WRB_fourth_edition_2022-12-18.pdf.
- Jafarzadeh AA, Burnham CP. Gypsum crystals in soils. *Eur J Soil Sci.* 1992;43:409-20. <https://doi.org/10.1111/j.1365-2389.1992.tb00147.x>
- Karathanasis AD, Hajek BF. Revised methods for rapid quantitative determination of minerals in soil clays. *Soil Sci Soc Am J.* 1982;46:419-25. <https://doi.org/10.2136/sssaj1982.03615995004600020042x>

- Marengo JA, Bernasconi M. Regional differences in aridity/drought conditions over Northeast Brazil: Present state and future projections. *Clim Change*. 2015;129:103-15. <https://doi.org/10.1007/s10584-014-1310-1>
- Moore DM, Reynolds RCJ. X-ray diffraction and identification and analysis of clay minerals. Oxford: Oxford University Press; 1989.
- Neher RE, Bailey OF. Soil survey of white sands missile range, New Mexico. Washington, DC: National Cooperative Soil Survey; 1976.
- Neumann VHML. Geologia e recursos minerais da folha Poço da Cruz, SC.24-X-A-VI: Estado de Pernambuco e de Alagoas. Brasília, DF: CPRM; 2017.
- Pessoa LGM, Freire MBGS, Araújo Filho JC, Santos PR, Miranda MFA, Freire FJ. Characterization and classification of halomorphic soils in the semiarid region of northeastern Brazil. *J Agric Sci*. 2019;11:405. <https://doi.org/10.5539/jas.v11n4p405>
- Poch RM. Characteristics of the sand fraction of two hyper-gypsic horizons of 'El Pla d'Urgell' NE (Spain). *Egypt J Soil Sci*. 1992;31:523-35.
- Porta J. Methodologies for the analysis and characterization of gypsum in soils: A review. *Geoderma*. 1998;87:31-46. [https://doi.org/10.1016/s0016-7061\(98\)00067-6](https://doi.org/10.1016/s0016-7061(98)00067-6)
- Rasiah V, Armour JD, Menzies NW, Heiner DH, Donn MJ. Impact of pre-existing sulphate on retention of imported chloride and nitrate in variable charge soil profiles. *Geoderma*. 2004;123:205-18. <https://doi.org/10.1016/j.geoderma.2004.02.001>
- Reiss AG, Gavrieli I, Rosenberg YO, Reznik IJ, Luttge A, Emmanuel S, Ganor J. Gypsum precipitation under saline conditions: Thermodynamics, kinetics, morphology, and size distribution. *Minerals*. 2021;11:141. <https://doi.org/10.3390/min11020141>
- Ribeiro MR, Lima JFW, Oliveira LB, Souza Jr VS. Data from: Projeto - Solos de referência de Pernambuco – Perfil 26. Recife: Museu de Solos de Pernambuco Professor Mateus Rosas Ribeiro; 1998a [cited 2024 Apr 29]. Available from: <https://museudesolospe.com/index.html>.
- Ribeiro MR, Lima JFW, Oliveira LB, Souza Jr VS. Data from: Projeto - Solos de referência de Pernambuco – Perfil 27. Recife: Museu de Solos de Pernambuco Professor Mateus Rosas Ribeiro; 1998b [cited 2024 Apr 29]. Available from: <https://museudesolospe.com/index.html>.
- Richards LA. Diagnosis and improvement of saline and alkali soils. Washington, DC: United States Salinity Laboratory; 1954.
- Santos HG, Jacomine PKT, Anjos LHC, Oliveira VA, Lumberras JF, Coelho MR, Almeida JA, Araújo Filho JC, Oliveira JB, Cunha TJF. Sistema brasileiro de classificação de solos. 5. ed. rev. ampl. Brasília, DF: Embrapa; 2018.
- Santos RD, Lemos RC, Santos HG, Ker JC, Anjos LHC. Manual de descrição e coleta de solo no campo. 5. ed. rev. ampl. Viçosa, MG: Sociedade Brasileira de Ciência do Solo; 2015.
- Schaefer CEGR. Clima e paleoclima do Acre: Memórias e cenários da aridez quaternária na Amazônia e implicações pedológicas. In: Anjos LHC, Silva LM, Wadt PGS, Lumberras JF, Pereira MG, editors. Guia de Campo da IX Reunião de Classificação e Correlação de Solos. Brasília, DF: Embrapa; 2013. p. 59-81.
- Schaetzl RJ, Anderson S. Soils genesis and geomorphology. Cambridge: Cambridge University Press; 2005.
- Soil Survey Staff. Keys to soil taxonomy. 13th ed. Washington, DC: United States Department of Agriculture, Natural Resources Conservation Service; 2022.
- Vidal-Torrado P, Chiapini M, Cooper M, Villagran XS. Micromorfologia de solos da XIII Reunião Brasileira de Classificação e Correlação de Solos. In: Silva BM, Lumberras JF, Coelho MR, Oliveira VA, editors. Guia de Campo da XIII Reunião Brasileira de Classificação e Correlação de Solos: RCC do Maranhão. Brasília, DF: Embrapa; 2020. p. 320-83.
- Violante A, Pigna M, Ricciardella M, Gianfreda L. Adsorption of phosphate on variable charge minerals and soils as affected by organic and inorganic ligands. *Dev Soil Sci*. 2002;28:279-95. [https://doi.org/10.1016/s0166-2481\(02\)80057-5](https://doi.org/10.1016/s0166-2481(02)80057-5)

Wang L, Roy A, Tittsworth R, Seals RK. Mineralogy of soil susceptible to sulfate attack after stabilization. *J Mater Civ Eng*. 2004;16:375-82.
[https://doi.org/10.1061/\(asce\)0899-1561\(2004\)16:4\(375\)](https://doi.org/10.1061/(asce)0899-1561(2004)16:4(375))

Watson A. Gypsum crusts in deserts. *J Arid Environ*. 1979;2:3-20.
[https://doi.org/10.1016/S0140-1963\(18\)31700-2](https://doi.org/10.1016/S0140-1963(18)31700-2)

Watson A. Structure, chemistry and origins of gypsum crusts in southern Tunisia and the central Namib Desert. *Sedimentology*. 1985;32:855-75.
<https://doi.org/10.1111/j.1365-3091.1985.tb00737.x>

Yamnova IA, Golovanov DL. Morphology and genesis of gypsum pedofeatures and their representation on detailed soil maps of arid regions. *Eurasian Soil Sci*. 2010;43:848-57.
<https://doi.org/10.1134/s1064229310080028>